ON THE ROLE OF SATURATION TEMPERATURE IN THERMAL MANAGEMENT THROUGH TWO-PHASE MECHANICALLY PUMPED LOOP

M. Pedroza-Torres[1]*, R. Rioboo[2], V. Lemort[1]

[1] Thermodynamics Laboratory / Université de Liège, Liège, Belgium

[2] Euro Heat Pipes, Nivelles, Belgium

* *Corresponding Author: mptorres@uliege.be*

Abstract. The impact of commercial aviation on the volume of polluting emissions is a problem that has become more relevant over the years, from initiatives at a personal level such as abstaining from the use of aircraft, to approaches at a government level with the dissent via taxes in some countries, there have been various ways of facing a problem whose solution may possibly go through the path of technological development. In today's world, the growing demand for power in the transition to electric aviation systems brings together the need to improve the thermal management systems associated with their correct operation. It is in this context where flow boiling cooling technologies have demonstrated their potential for thermal management. This two-phase solution uses the latent heat of vaporisation as a resource in the extraction of heat, with low requirements in mass flow and near-isothermal operation, resulting in a low temperature difference between hot source and cold sink even for long distances where the addition of pumping stages becomes necessary. In the overall design scheme of a two-phase cooling circuit, adjusting the saturation temperature or mass flow of the coolant are control possibilities in the face of changing conditions of the heat transfer environment. This work presents a set of five criteria to establish a saturation temperature setpoint under steady state conditions. Two application examples are presented, and the results are compared with case studies of two-phase mechanically pumped loop (2ΦMPL) from the aerospace industry.

Keywords. Two-phase, MPL, Flow boiling, Temperature setpoint, Selection criteria.

Nomenclature

A	Area (m^2)
ρ	Density (kg/m^3)
μ	Dynamic viscosity (Pa.s)
R	Gas constant (J/kg.K)
$\dot{Q}$	Heat transfer rate (W)
h_{lv}	Latent heat of vaporisation (J/kg)
M	Mach number (-)
$\dot{m}$	Mass flow rate (kg/s)
P	Pressure (Pa)
T	Temperature (K)
h	Specific enthalpy (J/kg)
γ	Specific heat ratio (-)
v	Velocity
$\dot{V}$	Volumetric flow (m^3/s)

Subscripts

cs	Cross-section
l	Liquid
s	Saturation
snd	Sound
v	Vapour

Acronyms

FoM	Figure of Merit
HTC	Heat Transfer Coefficient
LPD	Low Pressure Drop
LVF	Low Volumetric Flow
RTC	Robust Temperature Control
2ΦMPL	Two-Phase Mechanically Pumped Loop

1 Introduction

Nowadays, there are few problems capable of bringing together so many countries in a common purpose as climate change does. The risks to civilisation and the ecosystem have become tangible over the years, leading to government regulations and initiatives from major technological players that are setting new lines of development [1].

In this regard, the aeronautical industry, committed to the goal of decarbonization [2], has expanded its investment and research horizons towards electrification, a growing market with power dissipation demands proportional to the size and performance of future aircraft [3] [4].

These initiatives bring new challenges in thermal management; the need to acquire, transport, and reject heat within complex structural configurations and high power density per unit area has shifted attention towards two-phase heat transfer solutions, taking advantage of the ability to absorb large amounts of heat by harnessing the latent heat of vaporisation [5] [6].

Passive thermal management alternatives such as heat pipes have demonstrated their capability and reliability over the years in the aerospace environment [7]. However, the mass budget required for use over long distances between heat acquisition and rejection points have shifted focus towards the development of systems with an added pumping stage, such as 2ΦMPLs. These systems allow a new level of control over mass flow, near-isothermal operating conditions, and the theoretical ability to extend their branches to the temperature control of parallel thermal loads. These intriguing capabilities come with numerous questions about the operational requirements of this technology [6].

This work presents a set of five criteria to establish a saturation temperature setpoint under steady state conditions. Two application examples are presented, and the results are compared with case studies on thermal control in the aerospace industry: 1) Telecommunication satellite (simulation results with ammonia) [8], and 2) Instruments for measurements in advanced physics (actual set-point selected for operation with carbon dioxide) [9].

2 Fundamentals of a 2ΦMPL

2.1 Basic Mechanics

A simplified representation of a single-loop 2ΦMPL intended for the thermal management of electronic components is shown in Figure 1a, accompanied by its typical behaviour on the pressure-enthalpy diagram (Figure 1b). The description of the operating principle of the loop starts at the accumulator which performs three functions in the configuration shown: 1) supplying liquid to the pump to prevent cavitation, 2) dampening transient excess flow caused by changing conditions in the evaporator, and 3) setting the minimum pressure level within the loop through the controlled activation of an electric heater. Downstream is the pump, which is responsible for maintaining the fluid flow within the system, overcoming pressure losses by increasing the mechanical energy of the flow. The next component is the evaporator, which acquires heat from the hot source while utilising the latent heat of vaporisation to maintain the near-isothermal condition in the working fluid. Finally, the heat is rejected in the condenser, where the working fluid returns to a subcooled condition to complete the cycle again at the accumulator.

a)

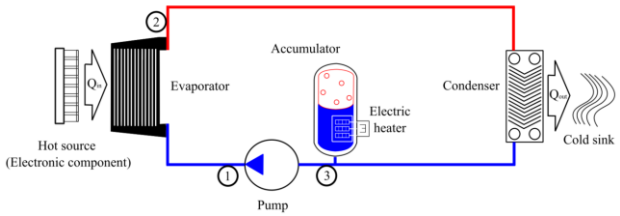

b)

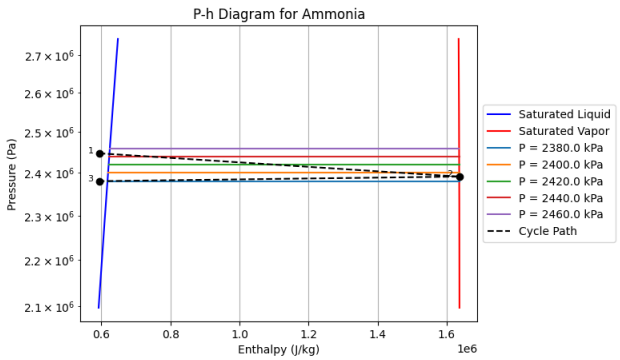

Figure 1: a) 2ϕMPL main components, b) Example of 2ϕMPL P-h diagram.

2.2 Control Strategies

Control strategies for 2ΦMPL systems are still an area under exploration, with thermohydraulic instabilities often occurring at both the component and system levels [10]. Flow restrictors and surface coatings have shown some of the best results in

reducing flow disturbances [11] [12] [13] [14]. However, the disparity in the response times between thermal and hydraulic dynamics makes it a challenging issue, leading to the consideration of heuristic control methodologies (black box approaches) [15]. For clarity in the explanation of the application example in this work, a simple strategy will be considered by setting a nominal temperature value in the working fluid, while response to disturbances will be managed through variations in pump speed.

3 Temperature Setpoint Selection Criteria

3.1 Higher HTC

Improvements in the heat transfer coefficient (HTC) achieved by operating at higher pressure levels have been reported by numerous authors in the phenomenon of flow boiling [16] [17] and can be seen in Figures 2 and 3. The physical argument behind this effect is the reduction in surface tension (due to the increase in saturation temperature), which leads to lower energy requirements for the extension of the liquid film needed for bubble formation. Additionally, operating at higher pressure levels results in smaller bubble sizes, leading to enhanced and more homogeneous nucleation flow. Therefore, according to this criterion operating at the highest possible pressure (saturation temperature) is the best option.

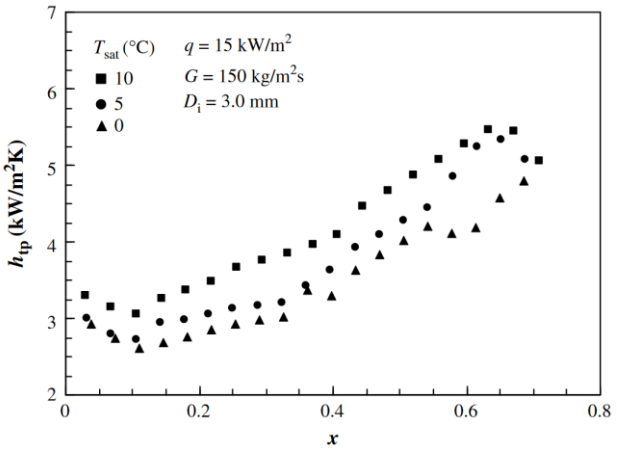

Figure 2: The effect of saturation temperature on heat transfer coefficient for propane **[16]**.

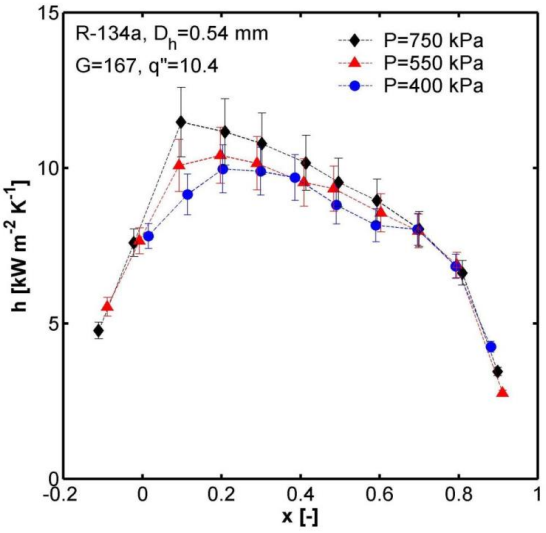

Figure 3: The effect of saturation pressure on the heat transfer coefficient for R-134a **[17]**.

3.2 Higher Latent Heat of Vaporisation

As discussed in the previous paragraph, while the heat transfer coefficient can benefit from setting higher pressure levels (saturation temperature) within the loop, operating in the upper region of the P vs h diagram is associated with lower values of latent heat of vaporisation (Figure 4), which reduces the range of the two-phase region and thus limits the spectrum of isothermal operation. Based on the criterion of high latent heat of vaporisation, it is suggested to operate at the minimum temperature (pressure) settled by the operational requirements of the thermal load.

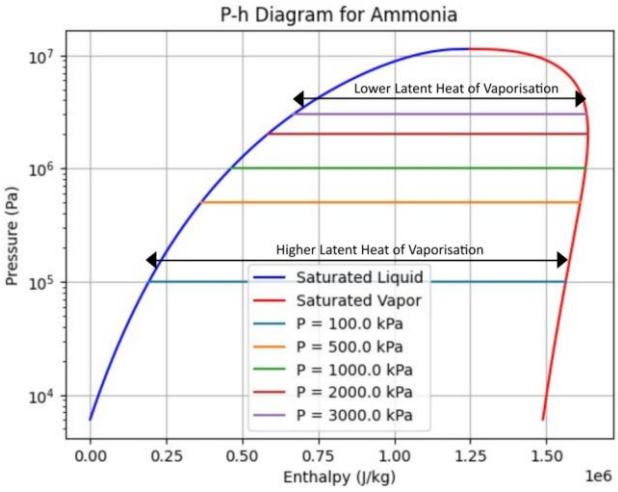

Figure 4: Example of P-h diagram.

3.3 *Robust Temperature Control*

For control purposes, it is beneficial to set a saturation temperature setpoint as close as possible to the critical temperature, where even with relatively large variations in the manipulated variable (pressure regulated from the accumulator), the changes in the controlled variable (saturation temperature) remain minimal [18]. This scenario of control robustness can be assessed by evaluating the gradient between pressure and temperature variations and selecting the temperature with the highest value as shown in Equation (1), based on the analysis of behaviour in the P vs T diagram of the working fluid (Figure 5).

$$T_{RTC\ criterion} = T_s|_{\max\left(\frac{dP}{dT}\right)} \tag{1}$$

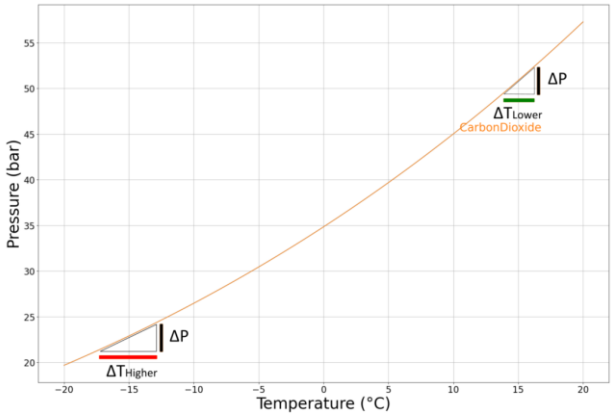

Figure 5: Example of P-T diagram.

3.4 *Lower Pressure Drop*

In a 1ΦMPL (based on sensible heat transfer) the ability to extract heat must be enhanced by increasing mass flow, however the use of latent heat means that for 2Φ-MPL less mass flow is required, and it is possible to reduce the diameter of the pipe, although this will increase the pressure losses. Gerner et al.'s proposal [19] demonstrates how certain formulations allow for distinguishing the contribution of factors in relation to pressure losses for turbulent flow in smooth-walled tubes. A single numerical value (called a Figure of Merit FoM) is proposed to quantify the relationship of multiple thermohydraulic properties. The aim would be to determine the saturation temperature that maximises the value of the Figure of Merit referred to as Low Pressure Drop (LPD FoM) in Equations (2) and (3), by calculating the thermohydraulic properties at that temperature depending on the chosen working fluid.

$$T_{LPD\ criterion} = T_s|_{\max\ (LPD\ FoM)} \tag{2}$$

$$LPD\ FoM = \frac{1}{\frac{\mu_l^{1/4}}{\rho_l (h_{lv})^{7/4}} + \frac{\mu_v^{1/4}}{\rho_v (h_{lv})^{7/4}}} \tag{3}$$

3.5 *Lower Volumetric Flow*

Equation (4) shows the definition of volumetric flow and its inverse relationship with respect to the product of liquid density by latent heat of vaporisation for turbulent flow in smooth-walled tubes [19]:

$$\dot{V} = \frac{\dot{m}}{\rho_l} = \frac{\dot{Q}}{\rho_l h_{lv}} \tag{4}$$

Returning to the concept of the Figure of Merit, it is possible to determine the temperature values that would result in a lower volumetric flow rate (LVF FoM) in Equations (5) and (6), which is directly linked to a reduced pumping requirement.

$$T_{LVF\ criterion} = T_s|_{\max\ (LVF\ FoM)} \tag{5}$$

$$LVF\ FoM = \rho_l h_{lv} \tag{6}$$

3.6 *Sonic Limit Check*

It is suggested that the selected temperature setpoint reduces the influence of compressibility effects, (pressure fluctuations, flow maldistribution, etc.) which would add complexity and difficulties to the thermohydraulic control of the system. Therefore, it is essential to ensure that the vapour velocity in the fluid remains within the subsonic flow category (Mach < 0.8). If not, the operating conditions should be redefined, or a new working fluid should be selected [18].

4 Application Examples

In the following section, the application of the different selection criteria will be demonstrated according to the flowchart shown in Figure 6, based on two case studies with different dissipation requirements for electronic equipment. In each case study, the selection will be made simultaneously for two fluids: Case #1 (R1234yf vs Carbon Dioxide), Case #2 (R1234ze(E) vs Ammonia) the first with potential for aeronautical use (R1234yf / R1234ze(E)), and the second as a reference for comparison, linked to space applications (Carbon Dioxide / Ammonia).

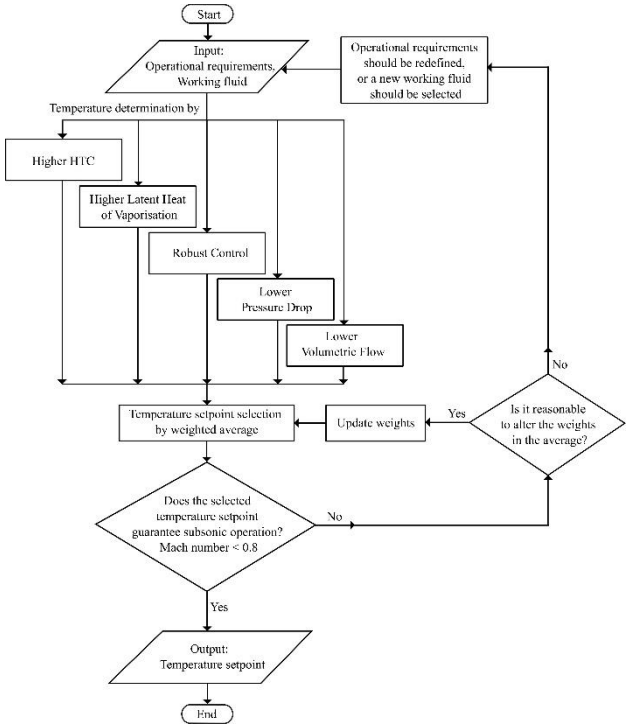

Figure 6: Temperature selection flowchart.

For the sake of simplicity in the explanation, the temperature range for the working fluid was taken as a reduction of the operational temperature requirement at hot source (by adding 5K to the lower limit and subtracting 5K from the upper limit). However, it is worth mentioning that a complete approach requires the estimation of the temperature deltas between fluid and hot source as a consequence of the convective resistance of the fluid, the conductive resistance of the evaporator material and the quality of the evaporator-heat source thermal contact interface.

4.1 Case study #1 (144 W)

In the context of advanced physics research, this first case study establishes some of the basic thermal management requirements for an in-orbit instrument specialised in antimatter detection [9], where the internal distribution of 8 silicon sheets capable of emitting electrical signals based on the impact of the particles under study is described. Around the 8 silicon planes detecting front-end electronics widely distributed at the periphery of the silicon planes (at no less than 192 locations) need to be very stable in temperature while dissipating 144 W of heat. The requirements of the first case study are summarised in Table 1.

Table 1: Operational parameters case study #1.

Power to be dissipated	144 [W]
Operational temperature requirement at hot source	-10 [°C] / 25 [°C]
Temperature range for the working fluid	-5 [°C] / 20 [°C]
Overall mass flow	2 [g/s]
Hydraulic diameter of the two-phase line	2.6 [mm]
Working fluid example (aeronautical application)	R1234yf
Working fluid for comparison (space application [9])	Carbon dioxide

4.1.1 Higher HTC: Figure 7 shows the choice of 20 °C for both R1234yf and Carbon Dioxide, according to the criterion of Higher HTC linked to operation at higher pressure levels.

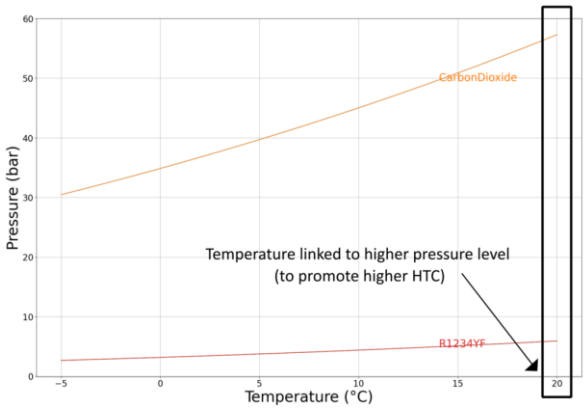

Figure 7: Case #1 (Higher HTC).

4.1.2 Higher Latent Heat of Vaporisation: Figures 8 and 9 shows the choice of -5 °C for both R1234yf and Carbon Dioxide, according to the criterion of Higher Latent Heat of Vaporisation linked to operation at lower pressure levels (lower temperatures).

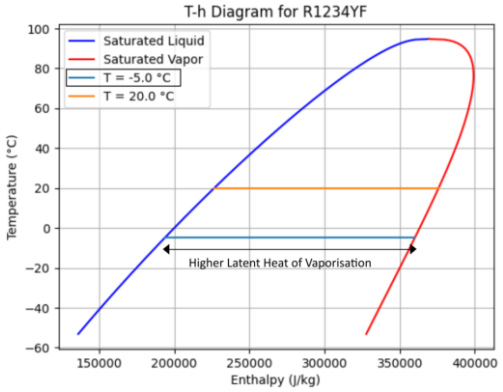

Figure 8: Case #1 (Higher Latent Heat of Vaporisation – R1234yf).

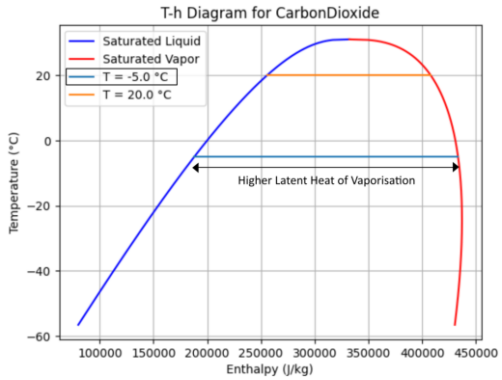

Figure 9: Case #1 (Higher Latent Heat of Vaporisation – Carbon dioxide).

4.1.3 Robust Temperature Control: Figure 10 shows the choice of 20 °C for both R1234yf and carbon dioxide, according to the criterion of Robust Temperature Control linked to operation at the point of largest gradient between pressure manipulation and temperature control.

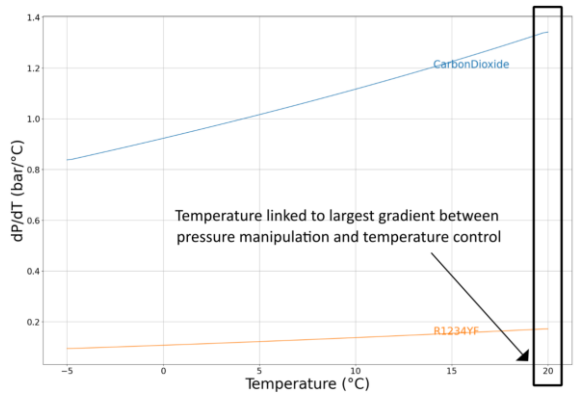

Figure 10: Case #1 (Robust Temperature Control).

4.1.4 Lower Pressure Drop: Figure 11 shows the choice of 20 °C for R1234yf and 2.5 °C for Carbon Dioxide, according to the criterion of Lower Pressure Drop for turbulent flow in smooth-walled tubes.

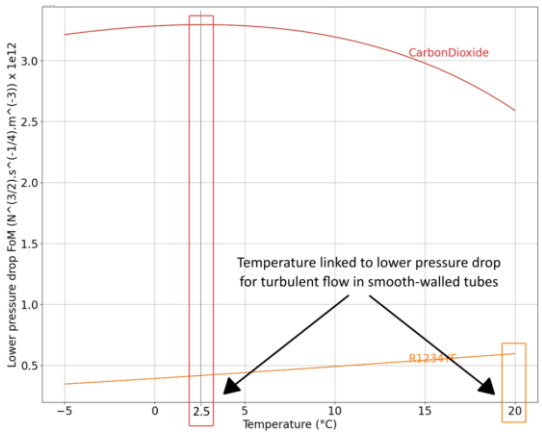

Figure 11: Case #1 (Lower Pressure Drop).

4.1.5 Lower Volumetric Flow: Figure 12 shows the choice of -5 °C for both R1234yf and Carbon Dioxide, according to the criterion of Lower Volumetric Flow with the purpose of reducing pumping power.

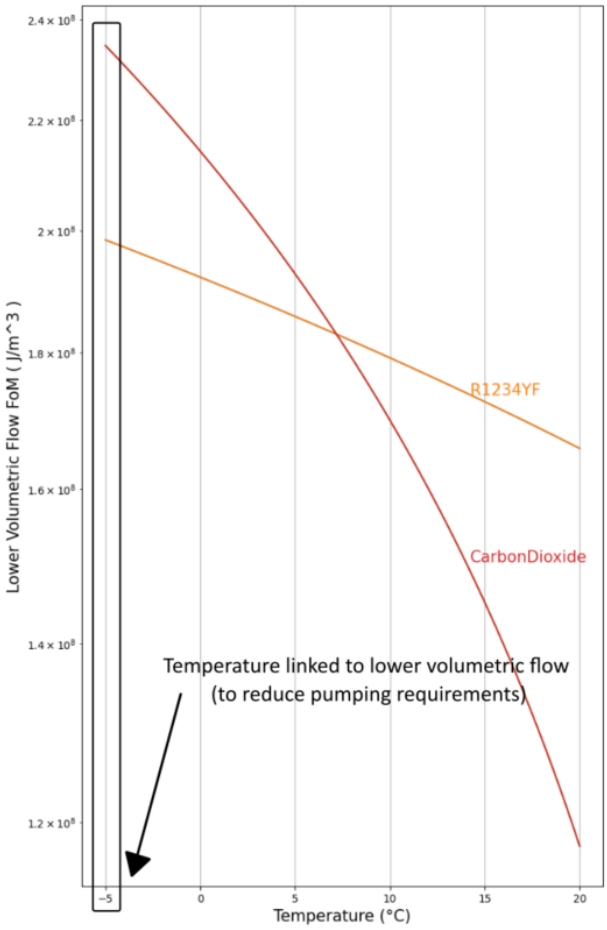

Figure 12: Case #1 (Lower Volumetric Flow).

4.1.6 Weighted average: Once the temperature values for each criterion have been obtained, the weighted average is calculated to determine the saturation temperature setpoint. In this context, two scenarios can be considered: a) known weights, and b) unknown weights.

a) Known weights scenario: Expert knowledge and operational decisions determine the values of the weights used to calculate the setpoint. In this context, various combinations of weights will position the saturation temperature in operating zones that may prioritise heat acquisition, prolong the intervals between interventions in the system, or achieve other objectives. Table 2 compares the temperature setpoints obtained for R1234yf and carbon dioxide for three different combinations of known weights, each serving a different purpose.

Table 2: Case study #1 (Setpoint selection – known weights scenario).

		Selected Temperature [°C]	
Criterion	Weight	R1234yf	Carbon Dioxide
Higher HTC	W1	20	20
Higher Latent Heat of Vaporisation	W2	-5	-5
Robust Temperature Control	W3	20	20
Lower Pressure Drop	W4	20	2.5
Lower Volumetric Flow	W5	-5	-5
Example 1: Equal weights (W1=W2=W3=W4=W5=0.2)			
Weighted average setpoint (Example 1)		**10**	**6.5**
Example 2: Greater heat acquisition (W1=0.7,W2=0.1,W3=0,W4=0.1,W5=0.			
Weighted average setpoint (Example 2)		**15**	**13.25**
Example 3: Less maintenance (W1=0.1,W2=0.1,W3=0.1,W4=0.3,W5=0.4)			
Weighted average setpoint (Example 3)		**7.5**	**`2.25**

b) Unknown weights scenario: In Equation 7 the number of different weight distributions 'N_{WD}' for 'n' indistinguishable objects (number of weight steps) among 'k' different parties (number of criteria) according to the stars and bars formula is equal to:

$$N_{WD} = \frac{(n+k-1)!}{(k-1)!\,n!} \tag{7}$$

Therefore, in the absence of specific weights, the construction of different weight distributions is proposed, after establishing the weight range and the step size for weight increments. As an example, step size for weight increments of 0.1 within the range 0 to 1 establishes $n = 10$ steps to cover the set of possible values $(0 \xrightarrow{Step\ 1} 0.1, \dots, 0.9 \xrightarrow{Step\ 10} 1)$, which assigned in $k = 5$ different positions establish a total of $N_{WD} = 1001$ possible combinations.

From here it is possible to calculate the weighted average associated with the different weight distributions, which gives N_{WD} candidate setpoint temperatures. Taking the set of possible values as a distribution, it is suggested to use the quartiles Q1, Q2 and Q3 as the lower value of the range, setpoint and upper value of the saturation temperature range respectively.

Returning to case study #1, the setpoint for the saturation temperature and its suggested range of variation are presented as a boxplot in Figure 13 for R1234yf and in Figure 14 for carbon dioxide.

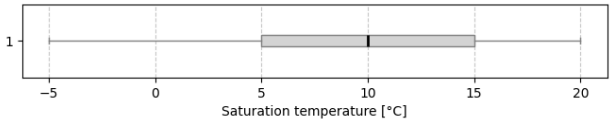

Figure 13: Case #1 (R1234yf setpoint selection – unknown weights scenario).

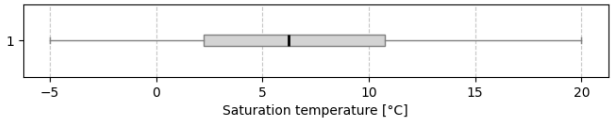

Figure 14: Case #1 (Carbon dioxide setpoint selection – unknown weights scenario).

4.1.7 Sonic Limit Check: At this verification stage it is first recommended to calculate the speed of sound using thermodynamic models and libraries available based on the fluid and temperatures of interest [20]. In the absence of such a resource, the formulation for ideal gases expressed in Equation 8 can be used as a calculation reference:

$$v_{snd} = \sqrt{\gamma \cdot R \cdot T} \tag{8}$$

The second step is to estimate the maximum velocity value developed in the line, for which a complete vaporisation scenario can be taken as a reference (vapor velocity), where the lowest density values for the gas phase will lead to maximum velocity values for an established geometry and mass flow in Equation 9:

$$v_v = \frac{\dot{m}}{\rho_v . A_{cs}} \tag{9}$$

The third and final step is to verify that the speed of the vapor flow remains far from the value of the speed of sound in that medium (to reduce the effects of compressibility) this can be achieved with calculated values less than 0.8 in the Mach number of Equation (10):

$$M = \frac{v_v}{v_{snd}} \tag{10}$$

The sonic limit check for case study #1 is summarized in Table 3 with properties obtained from the CoolProp 6.6.0 library [20].

Table 3: Case study #1 (Sonic Limit Check).

Working fluid	R1234yf			Carbon Dioxide		
Temperature setpoint range [°C]	{5;15}			{2.25;10.75}		
Quartiles	Q1	Median	Q3	Q1	Median	Q3
Temperature [°C]	5	**10**	15	2.25	**6.25**	10.75
Vapor velocity [m/s]	18.16	15.52	13.33	3.59	3.16	2.72
Mach number [-]	0.135	0.115	0.099	0.017	0.015	0.013
Vapour flow regime	Subsonic			Subsonic		

In this sense, the temperature setpoints proposed for the two fluids are far from the sonic limit, and are presented as a baseline for choosing a nominal operating point. For comparison purposes the accumulator setpoint chosen by the reference

2ΦMPL operating with carbon dioxide for thermal management of these dissipation requirements was 0 °C [9], a difference of less than 7 K with the median temperature of the unknown weight method shown above.

4.2 Case study #2 (6000 W)

Within the telecommunications satellite market, new requirements in the power required for signal processing (or in-orbit computing) are linked to increases in size and thermal dissipation requirements, with operating ranges that are increasingly similar to those of aeronautical applications, which has led to joint research programs between aeronautical and aerospace institutions [8]. Regarding this case study, three panels arranged inside a satellite assembly are designed to house 180 active electronic components with a combined dissipation requirement of 6000 W. The requirements of the second case study are summarised in Table 4, its setpoint selection (known weights) in Table 5, setpoint selection (unknown weights) in Figure 15 & 16 and its sonic limit check in Table 6.

Table 4: Operational parameters case study #2.

Power to be dissipated	6000 [W]
Operational temperature requirement at hot source	35 [°C] / 70 [°C]
Temperature range for the working fluid	40 [°C] / 65 [°C]
Overall mass flow	3.15 [g/s]
Hydraulic diameter of the two-phase line	9 [mm]
Working fluid example (aeronautical application)	R1234ze(E)
Working fluid for comparison (space application [8])	Ammonia

Table 5: Case study #2 (Setpoint selection – known weights scenario).

		Selected Temperature [°C]	
Criterion	Weight	R1234ze(E)	Ammonia
Higher HTC	W1	65	65
Higher Latent Heat of Vaporisation	W2	40	40
Robust Temperature Control	W3	65	65
Lower Pressure Drop	W4	65	65
Lower Volumetric Flow	W5	40	40
Example 1: Equal weights (W1=W2=W3=W4=W5=0.2)			
Weighted average setpoint (Example 1)		**55**	**55**
Example 2: Greater heat acquisition (W1=0.7,W2=0.1,W3=0,W4=0.1,W5=0.			
Weighted average setpoint (Example 2)		**60**	**60**
Example 3: Less maintenance (W1=0.1,W2=0.1,W3=0.1,W4=0.3,W5=0.4)			
Weighted average setpoint (Example 3)		**52.5**	**52.5**

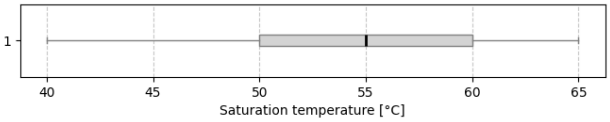

Figure 15: Case #2 (R1234ze(E) setpoint selection – unknown weights scenario).

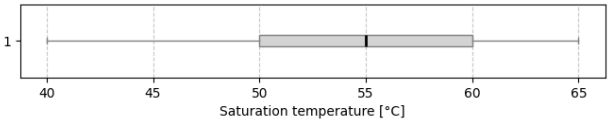

Figure 16: Case #2 (Ammonia setpoint selection – unknown weights scenario).

Table 6: Case study #2 (Sonic Limit Check).

Working fluid	R1234ze(E)			Ammonia		
Temperature setpoint range [°C]	{50;60}			{50;60}		
Quartiles	Q1	Median	Q3	Q1	Median	Q3
Temperature [°C]	50	**55**	60	50	**55**	60
Vapor velocity [m/s]	0.92	0.81	0.71	3.14	2.75	2.42
Mach number [-]	0.007	0.006	0.005	0.008	0.007	0.006
Vapour flow regime	Subsonic			Subsonic		

For comparison purposes the accumulator setpoint chosen by the reference 2ΦMPL prototype operating with ammonia for thermal management of these dissipation requirements was 51.56 °C [8], a difference of less than 4 K with the median temperature of the unknown weight method shown above.

5 Conclusions

- The five criteria presented: 1) Higher HTC, 2) Higher Latent Heat of Vaporisation, 3) Robust Temperature Control, 4) Lower Pressure Drop, 5) Lower Volumetric Flow, provide an analytical alternative for selecting a temperature setpoint that can be adjusted to the operational priorities of the case by modifying their weights in a weighted average formulation.
- In the case of selecting two different fluids for the same thermal management solution the chosen setpoint value may vary (case study #1) or remain the same (case study #2), depending on the behaviour of their thermodynamic diagrams and their performance based on the selected figures of merit.
- While the selection of nominal operating points must encompass the set of challenges in the construction, operation, and control of a 2ΦMPL, the approach presented above is proposed as a reasonable baseline.

Acknowledgement

This work has been made possible thanks to the MPL2030 project, a result of the collaboration between the Walloon government, the Skywin competitiveness cluster, the industrial partnership of Euro Heat Pipes - Calyos, and the academic collaboration between the University of Louvain and the University of Liège.

References

[1] J. Zhang, D. Ballas and X. Liu, “Global climate change mitigation technology diffusion: A network perspective,” Energy Economics, vol. 133, p. 107497, 2024.

[2] C. Jiang, T. D'Alfonso and J. Post, “Aviation decarbonization - Policies and technologies to support decarbonization of the aviation sector,” Transportation Research Part D: Transport and Environment, vol. 127, p. 104055, 2024.

[3] D. Sharar, N. R. Jankowski and B. Morgan, “Review of Two-phase Electronics Cooling for Army Vehicle Applications,” 2010.

[4] S. H. Lee, I. Mudawar and M. M. Hasan, “Thermal analysis of hybrid single-phase, two-phase and heat pump thermal control system (TCS) for future spacecraft,” Applied Thermal Engineering, vol. 100, p. 190–214, May 2016.

[5] Y.-G. Lv, Y.-T. Wang, T. Meng, Q.-W. Wang and W.-X. Chu, “Review on thermal management technologies for electronics in spacecraft environment,” Energy Storage and Saving, vol. 3, p. 153–189, 2024.

[6] J. v. Es and H. J. v. Gerner, “Benefits and Drawbacks of Using Two-Phase Cooling Technologies in Military Platforms,” 2011.

[7] T. Yang, T. Gao, S. Zhao and P. Zhang, "Performance Test of Novel Flat Capillary Pump Loop Heat Pipe under Anti-gravity and Microgravity," Microgravity Science and Technology, vol. 34, June 2022.

[8] J. Hugon, “Development of a Two-Phase Mechanically Pumped Loop (2ΦMPL) for the Thermal Control of Telecommunication Satellites,” 2008.

[9] J. v. Es, A. Pauw, G. van Donk, U. Ragnit, Z. He, B. Verlaat, C. Gargiulo, E. Laudi and P. van Leeuwen, “AMS02 Tracker Thermal Control Cooling System Test Results of the AMS02 Thermal Vacuum Test in the LSS at ESA ESTEC,” 2012.

[10] S. V. Garimella, A. S. Fleischer, J. Y. Murthy, A. Keshavarzi, R. Prasher, C. Patel, S. H. Bhavnani, R. Venkatasubramanian, R. Mahajan, Y. Joshi, B. Sammakia, B. A. Myers, L. Chorosinski, M. Baelmans, P. Sathyamurthy and P. E. Raad, “Thermal Challenges in Next-Generation Electronic Systems,” IEEE Transactions on Components and Packaging Technologies, vol. 31, p. 801–815, 2008.

[11] A. Koşar, C.-J. Kuo and Y. Peles, “Suppression of Boiling Flow Oscillations in Parallel Microchannels by Inlet Restrictors,” Journal of Heat Transfer-transactions of The Asme - J HEAT TRANSFER, vol. 128, March 2006.

[12] G. Hedau, R. Raj and S. K. Saha, “Complete suppression of flow boing instability in microchannel heat sinks using a combination of inlet restrictor and flexible dampener,” International Journal of Heat and Mass Transfer, vol. 182, p. 121937, 2022.

[13] K. C. Leong, J. Y. Ho and K. K. Wong, “A critical review of pool and flow boiling heat transfer of dielectric fluids on enhanced surfaces,” Applied Thermal Engineering, vol. 112, p. 999–1019, 2017.

[14] V. Y. S. Lee, G. Henderson, A. Reip and T. G. Karayiannis, “Flow boiling characteristics in plain and porous coated microchannel heat sinks,” International Journal of Heat and Mass Transfer, vol. 183, p. 122152, 2022.

[15] T. Zhang, J. T. Wen, Y. Peles, J. Catano, R. Zhou and M. K. Jensen, “Two-phase refrigerant flow instability analysis and active control in transient electronics cooling systems,” International Journal of Multiphase Flow, vol. 37, p. 84–97, 2011.

[16] K.-I. Choi, A. S. Pamitran, J.-T. Oh and K. Saito, “Pressure drop and heat transfer during two-phase flow vaporization of propane in horizontal smooth minichannels,” International Journal of Refrigeration, vol. 32, p. 837–845, 2009.

[17] S. S. Bertsch, E. A. Groll and S. V. Garimella, “Effects of heat flux, mass flux, vapor quality, and saturation temperature on flow boiling heat transfer in microchannels,” International Journal of Multiphase Flow, vol. 35, p. 142–154, February 2009.

[18] ADVANCED COOLING TECHNOLOGIES, “Pumped Two-Phase Fluid Selection,” 2024. [Online]. Available: https://www.1-act.com/thermal-solutions/active/pumped-two-phase/.

[19] H. J. v. Gerner, R. C. Van Benthem and J. v. Es, “Fluid selection for space thermal control systems,” in 44th International Conference on Environmental Systems, 2014.

[20] I. H. Bell, J. Wronski, S. Quoilin and V. Lemort, “Pure and Pseudo-pure Fluid

Thermophysical Property Evaluation and the Open-Source Thermophysical Property Library CoolProp," Industrial & Engineering Chemistry Research, vol. 53, p. 2498–2508, 2014.